



Hydrometallurgical recovery of zinc from industrial hot dipping top ash

Ewa RUDNIK

Faculty of Non-ferrous Metals, AGH University of Science and Technology,
Al. Mickiewicza 30, 30-059 Cracow, Poland

Received 8 September 2019; accepted 16 March 2020

Abstract: Top ash from hot-dip galvanizing plant was investigated as a source of secondary zinc to be returned to galvanizing bath. The waste material contained 63% Zn as metallic, oxide and hydroxychloride phases. It was leached in H_2SO_4 solutions (20% and 25%) at various bath loadings (100–300 g/L). Leaching behaviors of zinc, manganese, iron and chloride ions were investigated. A few strategies of iron elimination from leaching liquors were examined. Flocculant addition was harmful for subsequent filtration of iron precipitates due to increased viscosity of solution, while a combination of zinc oxide and calcium carbonate for rising pH resulted in the formation of dense suspension unenforceable to separate from zinc sulphate solution. Zinc electrowinning was carried out at different pH (from –0.5 to 2.8) using a range of current densities (3–10 A/dm²). Optimal conditions for pure metal recovery were: leaching in 20% H_2SO_4 solution at zinc ash content 100–150 g/L, $Fe_2O_3 \cdot xH_2O$ precipitation using H_2O_2 and $CaCO_3$, zinc electrowinning at pH of 0.1–1.0 at 3–6 A/dm². Correlations between pH and free H_2SO_4 concentration in electrolyte solutions were also discussed. pH–acid concentration dependence for zinc electrolyte was between experimental and calculated curves for pure H_2SO_4 solutions, while the curve was shifted towards lower pH if ferric ions were in the solution.

Key words: top ash; zinc; leaching; purification; electrowinning; recycling

1 Introduction

Hot dipping is a formation of protective metallic layers by immersion of a metal substrate into molten coating metal. Steel and iron are typically covered objects, while common coating materials are zinc, aluminum, tin and lead. Application of zinc for corrosion protection of ferrous substrates is called hot-dip galvanizing. It is realized at a temperature close to 450 °C by using batch or continuous processes [1]. The first method involves cleaning steel objects (pipes, fasteners, structures etc.), applying flux (a mixture of zinc and ammonium chlorides) to the surface, and then immersing the items in a molten bath of zinc to grow a thick coating. In turn, continuous galvanizing consists of unwinding coils of cold-rolled steel and feeding the sheet incessantly

through a cleaner, an annealing furnace, and then putting into a molten zinc bath to produce a protective layer.

Hot-dip galvanizing, like other industrial processes, generates some wastes. They are formed inside or on a surface of the molten zinc bath [1]. Hard zinc (bottom dross or hard spelter) consists of zinc–iron intermetallic phases [2,3] settling on a bottom of the galvanizing kettle. It is removed manually every 5–10 production days to prevent worsening optical and mechanical quality of the zinc-coated goods [4,5]. Zinc ash (skimmings) floats on the bath surface as a powdery product of a reaction of the molten metal with air oxygen. It is composed mainly of oxides as well as chlorides and sulphides originating from the pre-treatment stages [1]. Iron–aluminum intermetallics can also accumulate on the bath surface as so-called top dross when zinc–aluminum alloy is used [6]. The

zinc ash is skimmed continuously by workers before the galvanized objects are removed from the bath to avoid adhering the powder to the fresh coating and thus decreasing visual quality of the final product [1,4].

The waste materials contain high percentage of zinc, i.e. 95%–98% in the bottom dross [1,3–6] and 60%–90% in the zinc ash [1,4,7], being valuable sources of secondary metal. It was estimated that treatment of 1 t of steel generates about 10 kg of the zinc dross and 9 kg of the zinc ash, giving total zinc stream of 15–18 kg potentially to recover [4]. Statistical data show that every year in the European Union about 19 kg of steel per inhabitant is galvanized. For comparison, the average values calculated per inhabitant reach 12 kg in Poland, 26 kg in Belgium and 32 kg in Austria [8]. The Hot-dip Galvanized Steel Market report forecasts continuous increase in global production of galvanized steel at a compound annual growth rate of 5.1% in a period of 2019–2025 [9]. This indicates that the waste materials generated in galvanizing plants can exhibit desired and worthy sources of recoverable zinc, especially that both hard zinc and zinc ash are claimed as not dangerous goods.

Bottom dross formation represents 7%–11% of zinc consumption during galvanizing; however, it is not possible for galvanizers to recycle their dross to recover some of zinc. Therefore, it is sold at 65%–75% of zinc price to pyrometallurgical recycling plants [5,6,10]. In turn, the generation of the top ash is usually at a level of 15%–20% of zinc utilization and its worth reaches 35%–45% of the metal price [10–12]. In a contrast to the zinc dross [5,6], the zinc ash consists of easy leachable components suitable for hydrometallurgical treatment.

Leaching of the zinc ash is realized usually in aqueous solutions of sulphuric [12–15] or hydrochloric [16,17] acids, while alkaline leaching has been used to a less extend [18]. Hydrochloric acid is well-suitable and high-effective agent due to its aggressive action on the chlorine-containing ash, but chloride electrolytes are fairly problematic during subsequent metal electrowinning [19]. Sulphuric acid is the most common and cost-effective leachant for zinc-containing resources owing to good solubility of zinc sulphate. It reacts with metal, oxide, oxychloride, hydroxide-type and

other zinc compounds identified in the top ashes, being proper candidate for the leaching agent. In turn, caustic soda can dissolve zinc compounds, leaving iron impurities in the solid residues, but its applicability can be limited by crystallization of secondary products [20].

It is noticeable that although the hot-dip galvanizing is a widespread industrial process, only about twenty scientific sources devoted recycling of the zinc ash were cited by Web of Science data base for last fifty years. Most of the researches are related to hydrometallurgical treatment of the zinc ash and focus on the leaching with diluted H_2SO_4 (10%) [12–14]. Less often, further processing of the leachate via purification steps or zinc carbonate precipitation followed by zinc electrowinning was reported [13,21]. In the previous studies [14,15,21] detailed analyses of various zinc ashes and behavior of metallic impurities during the leaching were discussed. The aim of the current research was to evaluate rationality of one-stage production of zinc sulphate solution with high concentration by application of more concentrated sulphuric acid (20%–25%) and various contents of the waste material (100–300 g/L). Simultaneously, transfer of main metallic contaminants (iron, manganese), chlorine leachability in water and acid as well as acid consumption were examined. Dissolution stage was followed by solution purification using few precipitation strategies and subsequent zinc electrowinning at different current densities using electrolytes of various pH. The final product can be used again in hot-dip galvanizing.

2 Experimental

2.1 Top ash examination

Top ash was collected in an industrial galvanizing plant and screened to remove metallic zinc lumps, leaving oxide fraction called further the zinc ash. The powder was used in this investigation in a form as received.

The morphology of the ash was observed with a scanning electron microscope (SEM, Hitachi). General and detailed analysis of the elemental composition was performed using energy dispersive X-ray spectroscopy (EDS). For comparison, 1 g sample was dissolved in 100 mL 30% HNO_3 solution and concentrations of metal ions were determined by means of an atomic absorption

spectrometer (AAS Solaar M5, ThermoElemental). Phase composition of the zinc ash was determined using an X-ray diffractometer (Rigaku MiniFlex, Cu K_{α} radiation).

Two analytical methods were used for determination of metallic zinc concentration in the ash. Volumetric measurements were executed by agitation (a magnetic stirrer) of 1 g powder samples with 400 mL 20% H_2SO_4 with simultaneous collection of evolved hydrogen in a gaseous burette. Total volume of the gas was read after measurement was completed and recalculated into mass fraction of the metal.

Wet chemical analysis was based on a zinc cementation reaction followed by dissolution of cemented copper by Fe(III) salt and manganometric titration of ferrous ions. For this purpose, 1 g ash sample was agitated (a magnetic stirrer) with 10 mL 0.5 mol/L $CuSO_4$ for 15 min. Then, 10 mL 0.5 mol/L $(NH_4)_2SO_4 \cdot Fe_2(SO_4)_3$ was added and the solution agitation was continued for 10 min. Afterwards, 25 mL 20% H_2SO_4 , 50 mL Zimmermann–Reinhardt mixture and 200 mL H_2O were added. The obtained sample was titrated with 0.03 mol/L $KMnO_4$.

The concentration of soluble chlorine in the zinc ash was also found. 5 g powder samples were leached with 200 mL deionized water for 5 h at ambient temperature or 50 °C. After washing and solid phase separation (filtration) were completed, the filtrates were collected and diluted to 250 mL. 20 mL samples of the final solutions were titrated with 0.1 mol/L $AgNO_3$ using a conductometer (Crison MultiMeter) for tracking ionic conductance.

All titration procedures were carried out at an ambient temperature.

2.2 Zinc ash leaching

The zinc ash was leached in ambient conditions. 200 mL 20% or 25% H_2SO_4 and 100–300 g/mL powder were used. The suspensions were agitated with a magnetic stirrer (400 r/min). Leaching time was 120 min. A temperature of the bath was monitored during the process. 2 mL electrolyte samples were taken periodically to determine concentrations of metallic ions by AAS. Solid residues of the leaching were separated by gravity filtration, dried to a constant mass and weighed. XRD analysis of the solids was done.

pH of the solutions was measured (Crison

MultiMeter) before and after the leaching. Concentration of free H_2SO_4 was also determined by alkalimetric titration of 1 mL samples with 0.1 mol/L NaOH using methyl orange as an indicator. Concentration of chloride ions in the leachate was determined by conductometric titration using 0.1 mol/L $AgNO_3$.

Thermal effects of the leaching were estimated using calorimetric method. Measurements were performed using isolated glass container equipped with a magnetic stirrer (400 r/min). Portion of the ash (150–300 g/L) was added to 200 mL 20% H_2SO_4 of known mass and initial temperature. The temperature (± 0.1 °C) of the system was monitored every 15 s. A temperature increase ΔT required to evaluate the heat released during reaction was determined graphically. The heat effect Q was calculated with the formula:

$$Q = \frac{(m_G c_G + m_A c_A) \Delta T}{m} \quad (1)$$

where m_G is mass of isolated glass reactor, g; m_A is mass of acid solution, g; c_G is specific heat capacity of glass, 0.75 kJ/(kg·K) [22]; c_A is specific heat capacity of 20% H_2SO_4 solution, 3.53 kJ/(kg·K); m is mass of system [22].

2.3 Leachate purification

The solutions obtained after the leaching stage were purified from iron ions using precipitation methods. 100 mL of the solution agitated with a magnetic stirrer (400 r/min) was heated to (60 ± 2) °C, and then portions of 3% or 30% H_2O_2 were dropped to oxidize Fe^{2+} to Fe^{3+} ions.

A required amount of oxidizing agent was calculated according to the concentration of iron ions and added with 15% excess. The agitation of the solution was continued for 40–45 min. Then, portions of 10 mol/L NaOH solution or $CaCO_3$ powder were added to neutralize free acid, increase pH to 4.4 ± 0.1 and, thus, achieve hydrolytic precipitate of $Fe_2O_3 \cdot xH_2O$. The experiments with NaOH were carried out at a room temperature or (55 ± 5) °C. Precipitated suspension was cooled to an ambient temperature and 1%–4% (volume fraction, relative to the suspension volume) of Scanpol-51 flocculant solution (2 g/L) was added during intensive agitation (1000 r/min). The suspension was further slowly agitated (200 r/min) for 50–60 min to promote clumping particles of

hydrated iron oxide. After flocculation step was completed, the solid phase was filtered using laboratory vacuum filtration system. Precipitation with CaCO_3 was executed at a temperature of 60 or 80 °C. After pH adjusting, the solid phase was separated by vacuum filtration.

Another precipitation test was realized by an oxidation of Fe^{2+} with H_2O_2 or MnO_2 (0.5 g/L) followed by partial alkalization of the solutions with ZnO to pH of 4.0 and final alkalization with CaCO_3 to pH of 4.8 ± 0.1 .

After phase separation, pH of the filtrate was controlled and concentrations of metal ions were determined by AAS. Phase analysis of the solid phases was executed.

2.4 Zinc electrowinning

Electrowinning was conducted for 30 min at an ambient temperature. 100 mL of the electrolyte containing (70 ± 5) g/L Zn^{2+} , (1.0 ± 0.2) g/L Mn^{2+} and (7.0 ± 1.5) g/L Cl^- was used. pH of the solution was in a range from 1.0 to -0.5 . Initial H_2SO_4 concentration in the electrolyte was determined by titration of 1 mL samples with 0.1 mol/L NaOH in the presence of methyl orange. The electrolyte was agitated with a magnetic stirrer (200 r/min). Lead anode and aluminum cathode were used (each 3 cm × 3 cm). Cathodic current densities in a range of 3–6 A/dm² were applied. Voltage of the electrolysis was monitored and then used for

calculation of energy consumption per 1 kg of deposited metal. For comparative purposes, some experiments with more alkaline solutions (pH 2.0–2.8) or higher current densities (8–10 A/dm²) were performed. The cathodic deposits were observed under optical microscope (Nikon), while their phase composition was analyzed by X-ray diffractometry.

All measurements described above were realized at least twice and in ambient conditions (atmospheric pressure, and (21 ± 1) °C except as indicated).

3 Results and discussion

3.1 Zinc ash composition

The zinc ash was a grey powdery mixture of metallic and non-metallic phases. Particles with various dimensions from about 10 to about 150 μm were characterized with a rough surface composed of plate-like structures (Fig. 1).

General elemental composition was identified using energy dispersion spectrometry (EDS). The ash samples were tightly fixed in a conductive graphite resin to prepare compact and dense specimens. The EDS analyses were executed for five different areas, each of about 3.6 mm². For comparison, wet chemical analysis of the powder was implemented. Table 1 shows obtained results. It was found that results of both methods were quite

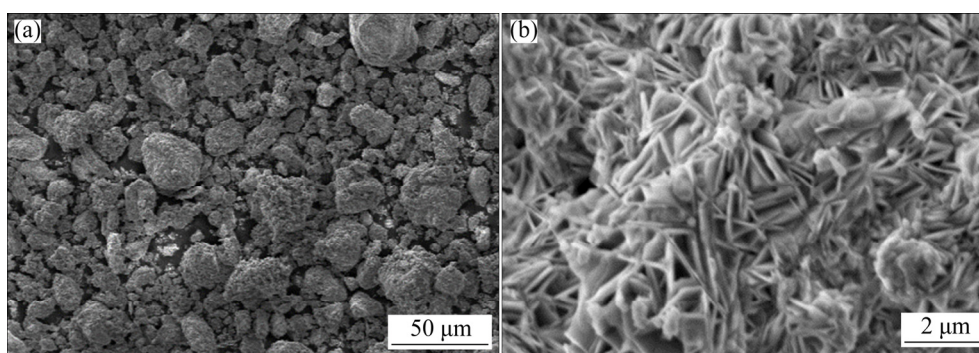


Fig. 1 SEM images of zinc ash powder: (a) Particles; (b) Surface of particles

Table 1 General compositions of zinc ash (wt.%)

Method	Zn	Fe	Al	Mn	Ca
EDS	64.88±3.66	0.85±0.09	1.66±0.23	0.59±0.01	0.30±0.07
AAS	62.74	1.02	1.70	0.49	0.38
Method	Si	O	Cl	S	C
EDS	0.45±0.45	19.31±0.26	8.10±0.24	0.07±0.02	6.32±1.37
AAS	–	–	–	–	–

comparable, indicating good preparation of the powdery material for the EDS examination. However, previous studies [21] showed some discrepancy of the composition data originated from non-uniformity of the material in a microscale and existence of solid residues after dissolution of the ash in sulphuric acid. The latter problem was eliminated in this study by the application of nitric acid for complete dissolution of the powder.

The zinc ash contained about 63% zinc, 1% iron, 1.7% aluminum and 0.5% manganese. No nickel, cobalt, copper and cadmium were detected. The EDS analysis indicated the presence of oxygen (about 19%) and chlorine (about 8%). The content of carbon seems to be uncertain due to the application of carbon-based resin. More detailed analysis executed at twenty various points of the samples showed some inhomogeneity of the material. It was found that the zinc content changed from about 48% to about 80%, with single particle having 95% Zn. The fluctuations of the zinc contents were accompanied by wide changes of the oxygen (1%–27%) and chlorine (1%–12%) contents. In turn, distribution of main metallic contaminants was quite uniform, i.e. 0.3%–2% Fe, 0.4%–2% Al and 0.2%–1.2% Mn. Low contents of the metallic impurities in the zinc ash revealed that this material was suitable for further hydrometallurgical metal recovery.

X-ray diffraction pattern (Fig. 2) showed the zinc ash as a mixture of three main phases: metallic Zn, zinc oxide (ZnO) and zinc hydroxychloride ($\text{Zn}_5(\text{OH})_8\text{Cl}_2 \cdot \text{H}_2\text{O}$) (simonkolleite). The existence of other compounds was not established due to their low contents in the material and detection limitations of the method.

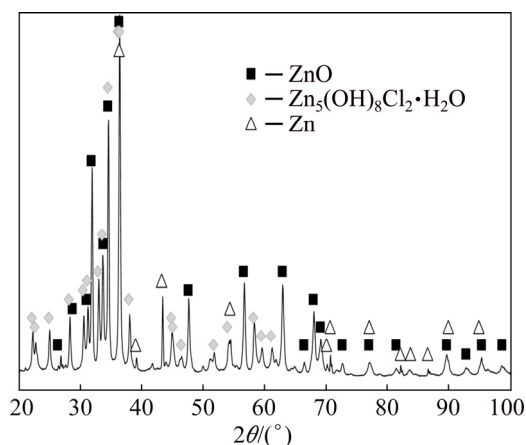


Fig. 2 XRD pattern of zinc ash

Content of the metallic phase was determined by using two chemical methods. The volumetric measurements indicated $(4.11 \pm 0.58)\%$ Zn, while the cementation combined with manganometric titration showed $(3.07 \pm 0.05)\%$ Zn. Both results are close, while the difference originates mainly from accuracies of the analysis methods. The volumetric experiments required a construction of rather simple system involving a gaseous burette and well-fitted reactor beaker. In such case, the main factor affecting the analysis accuracy was thorough immersion of the hydrophilic powder in the acid solution in the vessel enabling collection of all evolved gas in the burette. In turn, the second method was based on a sequence of the reactions running completely to obtain correct data.

Finally, the content of soluble chlorine in the ash was determined. It was found that a concentration of Cl^- ions in all aqueous solutions was at a level of about 0.75 g/L independent of the washing temperature. It corresponded to $(2.86 \pm 0.24)\%$ Cl removed from the zinc ash. This indicated that the water washing allowed to eliminate only about 35% of chlorine from the material, while the rest remained as insoluble compound, principally simonkolleite. Removal rates of $(0.86 \pm 0.11)\%$ Zn, $(0.05 \pm 0.01)\%$ Mn and 0.0008% Fe from the ash were also detected. Total mass losses of the water-washed samples were $(1.65 \pm 0.02)\%$. The comparison of the amounts of dissolved zinc and chlorine suggested that only residual flux was removed from the zinc ash during the water leaching.

The obtained results were related to other reports on chemical and phase compositions of the zinc ashes originating from galvanizing plants in different regions of the world. It was recognized that qualitative and quantitative compositions of the material are dependent mainly on the molten bath used, mode of galvanizing, type of steel and efficiency of metallic residues removal from the ash before its disposal. The latter can be realized by accumulation of the ash at the bath end, where is “chopped” (5%–10% Zn recovery), collection in a box placed at the bath kettle corner (30%–40% Zn recovery) or application of a rotating drum (50%–70% Zn recovery) [10]. Consequently, the content of metallic zinc in the ash can range from 62%–85% [4,7,18] to 6%–15% [13,21,23] after post-treating. It was also found that coarse fractions

of the zinc ash are enriched in zinc metal. For example, BAKARAT [7] showed that metallic zinc was the major constituent (76%) of the coarse fraction (+0.9 mm), while the fine grained fraction of the material (−0.9 mm) was depleted in the metal (64%). Similar tendency was observed for total zinc content. TAKÁCOVÁ et al [16] reported that a decrease in a particle diameter from +1.25 to −0.125 mm was accompanied by reduction of the zinc content from about 85% to about 63% at the average element content in the ash of about 78%. Simultaneously, fine grained fractions were gradually enriched in chlorine from about 13% to about 16%. Such behavior was confirmed by TRPČEVSKÁ et al [24], who observed decreased zinc (from 84% to 61%) and increased chlorine (from 14% to 25%) contents for particle diameters changed from +9.0 to −0.125 mm. Generally, the total chlorine content in the zinc ash is variable and can range from 1% [25] to 18%–28% [13,23,26], but is usually 5%–14% [4,14,15,17,23,24,27].

Phase analysis of the zinc ash confirms that three constituents Zn, ZnO and $Zn_5(OH)_8Cl_2 \cdot H_2O$ dominate in the material, independent of its origin [7,13,17,21,23]. However, some authors identified other zinc-containing phases like $Zn(OH)Cl$ [24], $Zn(ClO_4)_2 \cdot 6H_2O$ or/and $Zn_2OCl_2 \cdot H_2O$ [26] and $ZnCl_2$, $4ZnO \cdot ZnCl_2 \cdot H_2O$ [27]. Fractions of the particular components usually remain undefined, but DVOŘÁK and JANDOVÁ [13] found 63% $Zn_5(OH)_8Cl_2 \cdot H_2O$ and 31% ZnO from quantitative analysis of XRD data.

Basic zinc chlorides and zinc oxychlorides are hardly soluble in water [20], therefore chlorine is barely removable by simple washing. Moreover, the element can also exist in the ash as other insoluble compounds, for example, lead chloride [1,25] or basic aluminum chlorides [1,21]. GÜRESIN and TOPKAYA [25] reported that washing of the zinc ash of low chlorine content (1.4%) with distilled water or sodium carbonate solutions at 80 °C or 95 °C for 30 min at solid–liquid ratios between 1:2–1:10 removed about 80% Cl. This was confirmed by ŞAHIN et al [23], who eliminated about 94% Cl (1.75 mol/L Na_2CO_3 , S/L=1/5, 3 h, 80 °C) from the material containing initially 5% Cl. However, no metal loss during washing was declared. Despite of this, all data indicate that efficiency of the pre-treatment stage is greatly dependent on proportions of soluble to insoluble

chlorine-containing compounds in the waste.

Finally, it should be emphasized that other contaminants like lead, nickel, silicon, cadmium, iron, manganese, chromium, copper and arsenic are also detected in the zinc ashes [13,14,24,26]. They come from steel objects or molten baths containing alloying additives [10]. Their contents are usually about 1% or less, but their transfer to the solution during leaching can further affect efficiency of the electrowinning stage [15,28]. Therefore, detailed identification of the ash constituents is of great importance.

3.2 Zinc ash leaching results

Leaching of the zinc ash was carried out using two sulphuric acid solutions. Figure 3 shows exemplary kinetic curves for the dissolution of zinc, iron and manganese in 20% and 25% leachants. It was found that concentrations of metallic ions reached practically constant levels after 20–30 min of the process. This time was enough to dissolve zinc, while continuation of the process favored transfer of the impurities in some cases. The maximal leachabilities of iron and manganese were dependent on the amount of the material used and the acid concentration, but their quantities were quite similar (i.e. 0.4–1.4 g/L Fe^{2+} or Fe^{3+} and 0.4–1.8 g/L Mn^{2+}). The concentrations of iron and manganese ions were solely monitored because they are the most important contaminants in further processing of the solution. Iron ions, if not eliminated from the electrolyte, will decrease current efficiency of zinc electrowinning due to loop reactions: cathodic reduction of Fe^{3+} to Fe^{2+} [28] and anodic oxidation of Fe^{2+} to Fe^{3+} [29]. Mn^{2+} ions are oxidized on an anode surface, forming protective layer of MnO_2 [30]. In turn, aluminum ions are quite inert to electrode reactions in aqueous baths, thus their concentration is not tracked during the leaching stage. Calcium and silicon do not transfer to the acidic sulphate electrolyte due to formation of insoluble compounds [31].

Figure 4 summarizes the leaching behavior of the zinc ash. Good leachability of the waste originated from the presence of the compounds spontaneously reacting with sulphuric acid as indicated by thermodynamic calculations (Table 2). The final concentrations of the zinc ions increased from about 40 to about 120 g/L for enlarged loading

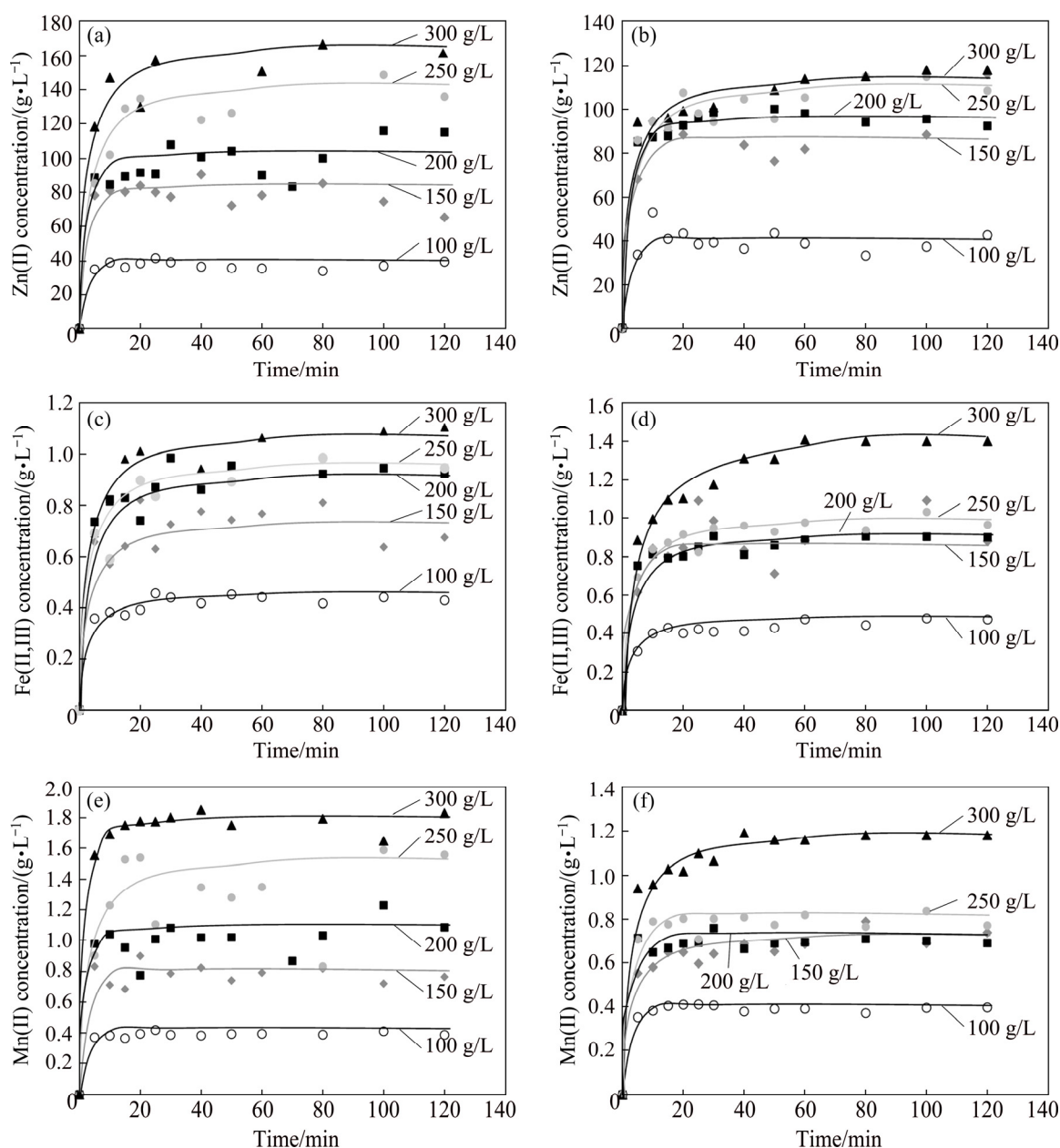


Fig. 3 Kinetic curves of metal leaching at different bath loadings in H_2SO_4 solutions with different concentrations: (a, c, e) 20%; (b, d, f) 25%

of the solution from 100 to 300 g/L, respectively (Fig. 4(a)). It was accompanied by gradual decrease in the leaching efficiency from about 80% to 65% (Fig. 4(b)). It was evidenced that the zinc transfer was practically independent of the acid concentration. However, the latter affected more obviously the amounts of the solid residue relative to the initial mass of the leached solid (Fig. 4(c)).

The 25% acid was theoretically sufficient to complete zinc recovery from the ash up to 250 g/L, especially the free acid remained in the leachate (Table 3). Due to no sufficient acid amounts, remainders of the initial ash components were

evidently detected in the residues (not shown). Unexpectedly, more filtration deposits were collected when the leaching was carried out in more concentrated solution at lower loadings (Fig. 4(c)). Diffraction analysis of the filtration residues indicated zinc salts like sulphate and chloride (Fig. 5). Both soluble salts crystallized in the secondary process during the filtration due to solution cooling. It should be emphasized that the ash leaching was accompanied by self-heating of the reacting system (Fig. 4(d)) owing to exothermic nature of the chemical reactions (Table 2). It was supported by calorimetric experiments showing the

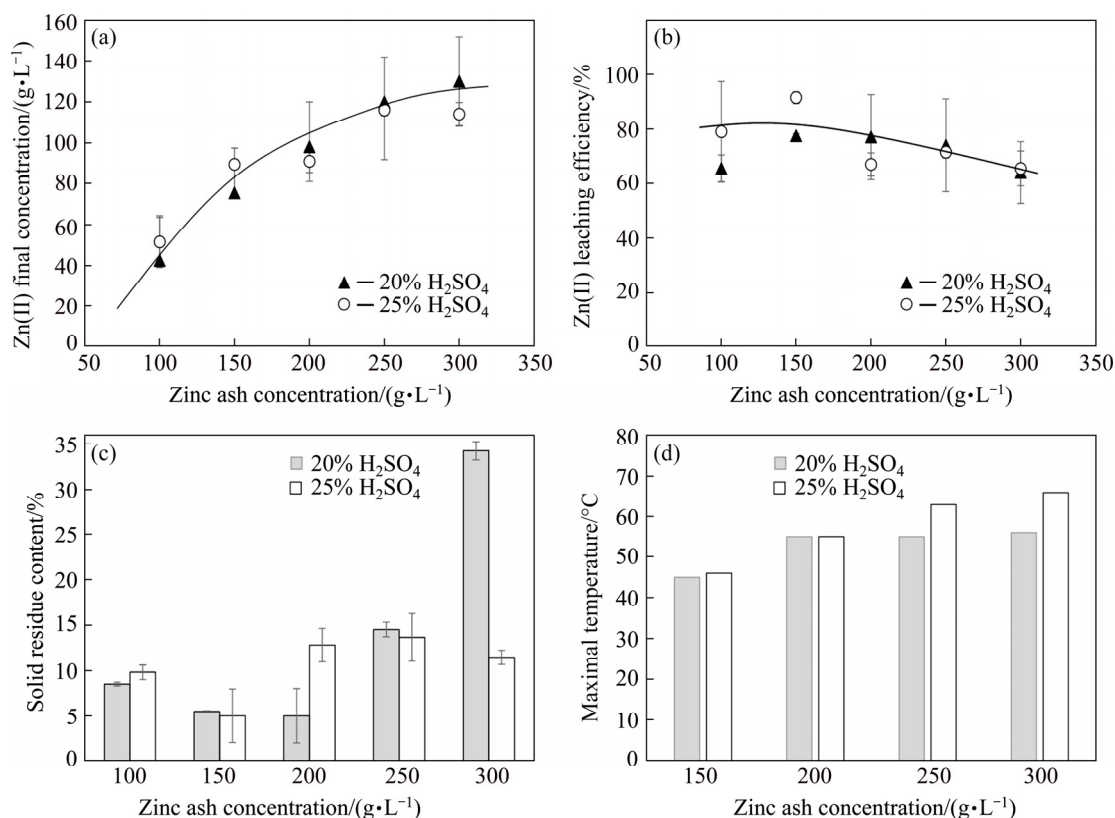


Fig. 4 Summary of zinc ash leaching: (a) Zn(II) final concentration; (b) Zn(II) leaching efficiency; (c) Solid residue content; (d) Maximal temperature

Table 2 Thermodynamic calculations related to dissolution of zinc phases (Basic thermodynamic data for 25 °C taken from Refs. [32,33])

Reaction	$\Delta G_r^\ominus /$ (kJ·mol ⁻¹)	$\Delta H_r^\ominus /$ (kJ·mol ⁻¹)
$\text{Zn} + 2\text{H}^+ = \text{Zn}^{2+} + \text{H}_2$	-147	-153
$\text{ZnO} + 2\text{H}^+ = \text{Zn}^{2+} + \text{H}_2\text{O}$	-64	-89
$\text{Zn}_5(\text{OH})_8\text{Cl}_2 \cdot \text{H}_2\text{O} + 8\text{H}^+ =$ $5\text{Zn}^{2+} + 2\text{Cl}^- + 9\text{H}_2\text{O}$	-106	Not obtainable*

* No thermodynamic data ΔH_r^\ominus for simonkolleite are available

heat released in a range from about -690 kJ/kg (150 g/L) to about -516 kJ/kg (300 g/L) for 20% H₂SO₄.

On one hand, the increase in the solution temperature enhanced solubility of zinc sulphate. However, the presence of sulphate ions of the acid influenced in an opposite way via “common-ion effect” [34]. The latter was more stressed when the solution temperature decreased during filtration, thus even washing of the solids with water was not totally effective. Therefore, despite of quite high solubility of zinc sulphate in pure water (550 g/L at

Table 3 pH and free H₂SO₄ concentrations in leaching liquors

Leaching condition		Leaching liquor	
H ₂ SO ₄ concentration/ %	Bath loading (zinc ash)/ (g·L ⁻¹)	pH	Free H ₂ SO ₄ concentration/ (g·L ⁻¹)
20 (211 g/L)	100	-1.09±0.07	121.2±4.7
	150	-1.02±0.08	81.4±9.4
	200	-0.61±0.02	35.5±1.7
	250	0.48±0.05	3.7±0.4
	300	3.06±0.01	1.0±0.1
25 (263 g/L)	100	-1.35±0.00	180.0±0.9
	150	-1.40±0.30	140.1±1.9
	200	-0.83±0.40	84.7±12.2
	250	-0.80±0.44	54.3±24.7
	300	-0.54±0.10	15.9±1.0

20 °C [22]) it cannot be considered irresponsibly if other ionic species exist in the solution [34].

The concentrations of free H₂SO₄ acid were determined in the final solutions (Table 3). It was realized by classical acid–base titration using small

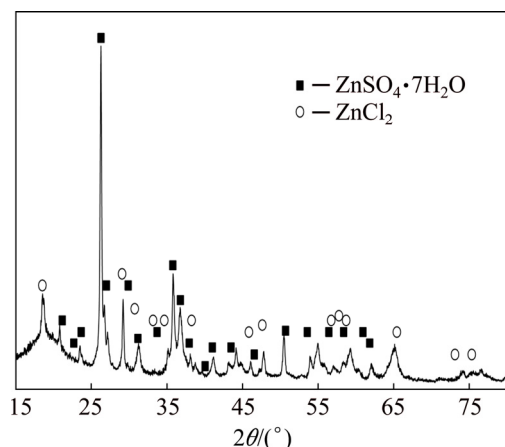


Fig. 5 XRD pattern of solid residues crystallized after leaching of 150 g/L zinc ash with 25% H_2SO_4

samples of the solution and methyl orange for detection of the end-point. The titration was completed when the indicator's color changed from red to orange corresponding to pH of 3.3 ± 0.1 . The pH regime of the final point was very important to prevent hydrolysis of ferric salts and obtain results of low errors [35]. For comparison, pH of the leaching liquors was determined. There was some correlation between the pH value and the acid concentration. However, evaluation of the data relative to the iron-free solution (electrowinning electrolyte) and pure acid solutions showed shifting the curve towards more acidic range (Fig. 6) which was caused by actual interference of ionic species occurring in the leaching liquors [38,39]. It seems that detection of the end-point with methyl orange was only slightly influenced by Fe(III) hydrolysis effects, while the experimental pH values were more dependent on ionic strength of solutions [40]. Acidity was established by using a combined glass electrode and a digital pH-meter. It shows pH by measuring a voltage of the electrochemical cell. Obviously, the cell voltage is dependent on activity (not concentration) of hydrogen ions influenced by ionic strength of the solution. High ionic strength solutions also change the liquid junction potential of the electrode. Moreover, the experimentally found pH values involved not only hydrogen ions coming from the acid dissociation, but also being generated during hydrolysis of the salts. To support the side effects on the electrode readings, the pH values of the pure acid solutions were determined. They were 0.02 and -0.04 for 20% and 25% solutions, respectively.

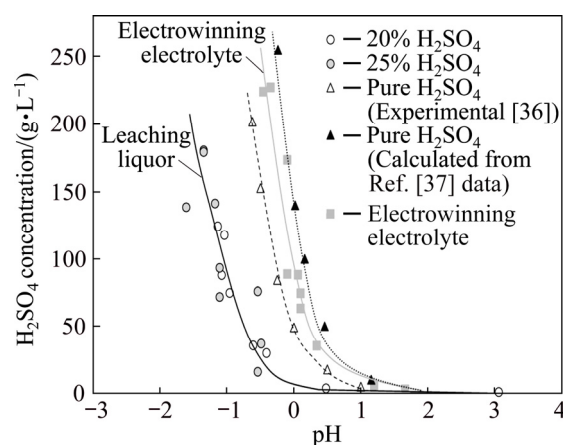


Fig. 6 pH– H_2SO_4 concentration correlations at 20 °C in solutions with ferric ions (leaching liquor), iron-free (electrowinning electrolyte) and pure acid [36] (Calculated pH values for complete first H_2SO_4 dissociation step and second dissociation degrees are approximately 0.34 taken from Ref. [37] at 20 °C)

It is necessary to state that analysis of free sulphuric acid in zinc sulphate solutions was investigated by several researchers [35,41]. The main problem remains a proper determination of the equivalence point, especially in the presence of some hydrolysable metal cations like Fe^{3+} and Al^{3+} of high concentrations. In such cases, complexing agents like EDTA, DCTA, their calcium and magnesium salts or reduction of Fe^{3+} to Fe^{2+} with potassium iodide were proposed to prevent spending NaOH titrant for hydrolysis processes instead of acid neutralization. The latter is extremely important when pH indicators like methyl red or phenolphthalein having pH of a color change of 4.8 and 8.2, respectively [41]. The current study showed that application of the indicator with lower color-change pH was more adequate to elude the hydrolysis effect.

The obtained data confirm gradual utilization of the acid for the ash dissolution and its incomplete consumption (Table 3). The only exceptions were for two highest bath loadings as expected from the theoretical predictions. In other cases, mutual equilibria between the ionic species and compounds in the ash resulted in an inability of the solid to react with the acid and falling solubility of the zinc salts.

The ash leaching transferred chlorine to the liquid phase. Amounts of chloride ions in the sulphate solutions were determined by method of

argentometric titration. The solubility of AgCl (1.6 mg/L) is highly reduced in comparison to Ag₂SO₄ (8 g/L) [22]. Moreover, AgCl precipitate in sulphate solution is additionally favored by “common-ion effect” [42]. Figure 7 shows final concentrations of chloride ions in the leaching liquors. Characteristic S-shaped dependencies were observed, indicating tendency of simonkolleite to react with sulphuric acid. The obtained values ranged from about 10 g/L in 20% H₂SO₄ to about 28 g/L in 25% H₂SO₄, being somewhat higher in some cases than those resulted from the chlorine content in the zinc ash. This discrepancy originated from a combination of analytical errors of the multicomponent powder by EDS and the solution by conductometric titration.

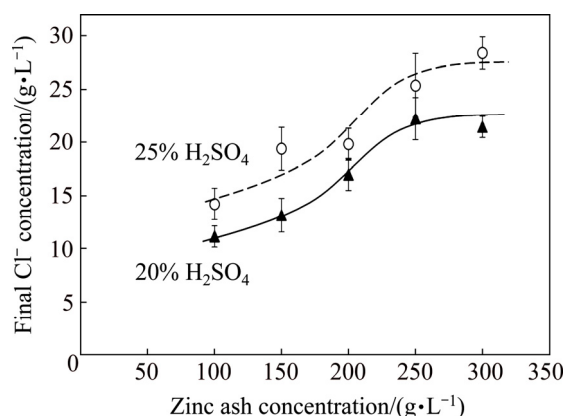


Fig. 7 Influence of H₂SO₄ concentration and zinc ash concentration on final Cl⁻ concentration in leachate

The existence of chlorine ions in the solution is disadvantageous, especially if electrowinning stage is planned to realize. Destructive action of the species is associated with corrosion of lead and aluminum electrodes [43], specifically in an interaction with manganese ions, and worsening quality of zinc deposits [44]. This may be overcome by elimination of the impurity before the electrolysis. Various methods were proposed to treat the zincous materials before the leaching or the solutions [23,24,45]. In this study, the water washing of the zinc ash (ambient temperature, solid-to-liquid ratio of 1:40, 120 min) was performed. It was followed by the leaching in 20% H₂SO₄ at the loadings of 50 and 100 g/L. Dissolution characteristics of the metal cations were the same as those of non-pre-treated material giving final concentrations of about 30 or 45 g/L Zn²⁺ at comparable Fe²⁺/Fe³⁺ and Mn²⁺ amounts of 0.2 g/L

(loading of 50 g/L) and 0.4 g/L (loading of 100 g/L). Solid residue contents were 7.6% for loading of 50 g/L and 11.1% for loading of 100 g/L. Since the water pre-treatment of the ash did not remove chlorine effectively and chloride ions still existed in the solution, further experiments were abandoned as not profitable.

Resuming the experiments it was concluded that good option of the leaching is using a bath loading of 150 g/L in 20% H₂SO₄ as the best compromise among expected final zinc sulphate concentration, leaching efficiency, consumption of the acid and crystallization of secondary products.

3.3 Leachate purification results

Leaching solutions were further purified from iron ions. Review of the literature data on iron elimination in zinc hydrometallurgy shows a variety of precipitation methods to produce jarosite, goethite or hematite, depending on the pH and temperature [46]. These methods are realized by an oxidation of Fe²⁺ ions using MnO₂ suspension [47], H₂O₂ solution [21,26] or O₂ (air) bubbling [48] as well as by combining action of the oxidants [49,50]. Afterwards, the solution pH is adjusted by calcium oxide [21] and hydroxide (lime) [50] or zinc oxide (zinc calcine, Waelz oxide) [13,46].

Few procedures were examined in this research. First of them involved oxidation of ferrous species by oxygen peroxide and raising the solution pH by concentrated sodium hydroxide solution to precipitate hydrated iron (III) oxide. The particles were then left for agglomeration by Scanpol-51. Scanpol-51 is a commercially available acryl-amide polymer intended for coagulation and flocculation of ferric precipitates in water purification and wastewater treatment. After required clumping time, the sediments were filtered, washed, dried and weighed.

Table 4 shows results of the precipitation combined with flocculant application. Despite the procedure was very effective for the removal of iron ions (usually to 0.2 g/L), the final results of the treatment were dependent on the additive amount and the zinc ion concentration. Addition of the flocculant strongly facilitated agglomeration of the precipitates and their sedimentation only at room temperature and specified clumping time. The conglomerates disaggregated when the solution temperature exceeded 30 °C or the flocculation time

was prolonged. Moreover, if the iron precipitation was realized at room temperature and high Zn^{2+} concentration, the flocculation product became gelatinous. This led to strong restraint of the filtration or its complete inhibition.

Generally, it is not recommended to use the flocculant for the solutions of high zinc sulphate concentration. Such solutions characterize with increased viscosity [51], resulting in a hindrance or prolonging the filtration stage. It further brings a secondary crystallization of zinc compounds like oxysulphate or zinc–sodium sulphate in a filter cake (Fig. 8) and increasing the filtrate pH up to 5.2–5.6. Hence, high losses of zinc ions (20%–50%) from

the solutions were obtained.

To avoid formation of any secondary zincous products, neutralization of the free acid was performed by addition of zinc oxide and then calcium carbonate to raise pH to the required level. Application of $CaCO_3$ seems to be advantageous due to additional agitation of the suspension by evolved carbon dioxide with simultaneous preventing additional contamination of the solution with calcium ions due to low solubility of $CaSO_4$ in zinc sulphate solutions [31,52]. Unfortunately, this revealed to be totally impractical since increasing zinc sulphate concentration highly increased the viscosity of the solution and led to the generation of

Table 4 Results of iron ions removal by NaOH followed by flocculation

H_2SO_4 concentration/ %	Bath loading (zinc ash leached)/ ($g \cdot L^{-1}$)	Flocculant content/ vol.%	Mass of precipitate/ g	Concentration before and after iron ions removal/($g \cdot L^{-1}$)					
				Zn(II)		Fe(II,III)		Mn(II)	
				Before	After	Before	After	Before	After
20	100	3	1.1	60	31	0.755	0	1.1	0.4
	100*	3	2.0	60	28	0.755	0.05×10^{-3}	1.1	0.2
	150	3	1.9	76	50	0.824	0.03×10^{-3}	1.0	0.7
	150*	3	1.8	76	43	0.824	0	1.0	0.5
	150	4	6.7	75	43	0.673	0.2×10^{-3}	1.0	0.9
	200	4	8.3	115	71	0.924	0.2×10^{-3}	1.1	1.0
	250	1	7.2	140	96	1.103	0.2×10^{-3}	1.6	1.2
	300	2	0.8	140	99	0.946	0.2×10^{-3}	1.8	1.4
25	150	2	–	88	51	0.879	0.2×10^{-3}	1.2	0.4
	200	3	6.2	95	78	0.899	0.9×10^{-3}	1.1	1.0
	250*	3	gel	114	88	1.037	0.01×10^{-3}	1.6	1.4
	300*	3	gel	116	–	1.408	–	1.2	–

* Fe(III) precipitation at ambient temperature

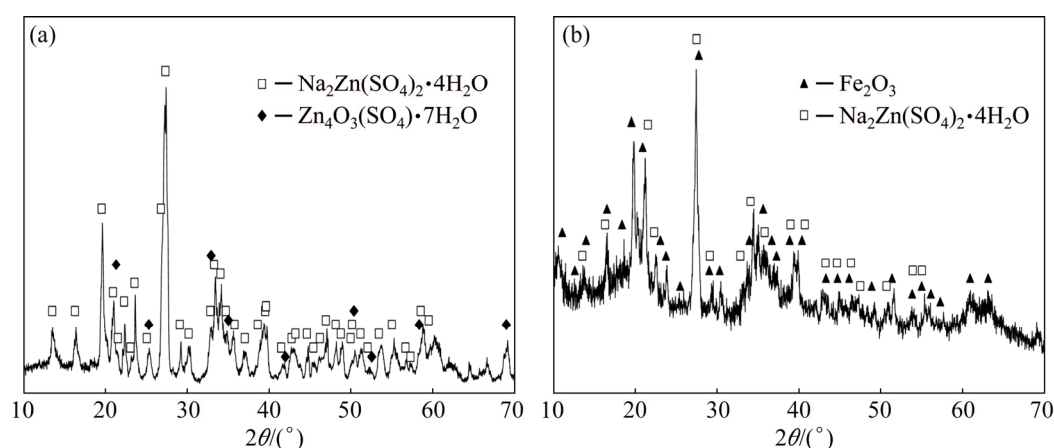


Fig. 8 XRD patterns of filter cakes after pH raising with NaOH followed by flocculant addition for zinc ash leaching in 20% H_2SO_4 solution at different bath loadings: (a) 100 g/L; (b) 200 g/L

calcium sulphate “pudding”. It made incapable of agitation of the dense suspension and subsequent phase separation by laboratory vacuum filtration system.

The last strategy involved addition of small portions of calcium carbonate to the solutions containing no more than 90 g/L Zn^{2+} . It resulted in the precipitation of calcium sulphate, facilitating adsorption of fine particles of hydrated iron oxide. The deposit was rather easy to filtrate, but losses of zinc ions were not avoided (8%–10% at initial 60–90 g/L Zn^{2+}) despite of the water-washing of the filter cake. Thus, the filter deposit consisted of gypsum, iron(III) oxide and basic zinc sulphate (Fig. 9).

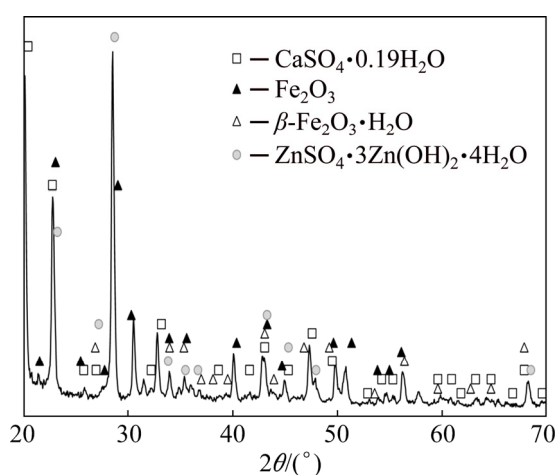


Fig. 9 XRD pattern of filter cake after pH raising with $CaCO_3$ for zinc ash leaching in 20% H_2SO_4 solution at bath loading of 150 g/L

The experiments showed that the satisfactory option of the solution purification was gradual addition of calcium carbonate. pH raising was accompanied by additional agitation of the suspension by the evolved gas. This procedure was more preferred than using calcium oxide powder or lime [21,50] due to prevention of formation of compact $CaSO_4$ film on the powder’s particles, thus inhibiting the reaction of the particle core with the acid. Moreover, despite of solid residue formation, this option was more preferred than using more expensive pure zinc oxide or Waelz oxide, being a new source of harmful chlorides and fluorides or other contaminants.

The purification stage demonstrated the impracticability of the concentrated zinc sulphate solutions obtained in the leaching stage. In such

systems secondary crystallization of zinc compounds was more enhanced, leading to high losses of zinc.

3.4 Zinc electrowinning results

The electrowinning was carried out using solutions acidified to various levels. Figure 6 shows pH– H_2SO_4 concentration correlation in the electrolytes purified from ferric ions. The results were close to the experimental dependence taken from the literature data [36]. Despite hydrolysis of zinc sulphate took place at pH above 6 [39,41] the application of methyl orange gave the results little different from the data for pure H_2SO_4 solutions. In turn, the pH– H_2SO_4 concentration dependence calculated according to the values of acid dissociation degrees found from spectroscopic studies [37] was shifted towards higher pH. All facts show that correlation between pH and free H_2SO_4 acid concentration in the aqueous solutions is difficult to determine in practice. Complicated nature of such analyses seems to originate from two-stage H_2SO_4 dissociation dependent on the acid concentration as well as occurrence of mutual ionic equilibria in the salt-containing electrolytes.

It was observed that a pH decrease from 1 to –0.5 was accompanied by a decrease in the current efficiency by about 10% from (94±1)% (Table 5). It was caused by a raising participation of hydrogen evolution in the cathodic processes. Simultaneously, improved electric conductance of the electrolyte by the acid addition reduced both electrolysis voltage (from 4.1 to 3.0 V) and energy consumption (from 4.6 to 3.9 kW·h/kg). All parameters were only slightly affected by the current densities due to relatively short duration of the electrolysis. Cathodic current efficiency, electrolysis voltage and energy consumption were similar to the values reported for the zinc electrowinning carried out in laboratory or industry scale [50,53]. It should be emphasized that the electrowinning effects are dependent not only on the concentrations of zinc sulphate and sulphuric acid, but also on current density, agitation rate and temperature [54,55]. These relationships are mostly evidenced for long-lasting electrolysis [55].

Pure zinc electrodeposits were gray and compact with uniform surface in a macroscopic scale. Microscopic examination revealed a morphology totally different from typical surfaces

Table 5 Results of zinc electrowinning

Solution pH	Current density/ (A·dm ⁻²)	Current efficiency/ %	Electrolysis voltage/ V	Energy consumption/ (kW·h·kg ⁻¹)
1.0	3	93.8	3.7	4.17
	4	92.9	4.0	4.63
	5	93.2	4.1	4.61
0.7	3	94.2	3.6	4.06
	4	94.8	3.7	4.14
	5	93.8	4.1	4.64
	6	94.5	4.0	4.50
0.1	3	91.5	3.5	4.06
	4	91.4	3.7	4.30
	5	95.2	3.8	4.24
	6	94.2	3.9	4.40
-0.2	3	87.7	3.1	3.75
	4	83.9	3.1	3.92
	5	88.2	3.2	3.85
	6	88.6	3.3	3.96
-0.5	3	80.2	3.0	3.97
	4	83.5	3.0	3.82
	5	84.3	3.1	3.91
	6	82.8	3.2	4.10

produced from acid sulphate baths where hexagonal platelets are usually observed [53,54]. The layers characterized with rough surfaces with randomly distributed pits at pH in a range of 1.0–0.1, independent of the current density (Figs. 10(a) and (b)). The surface became more even for more acidic solutions, i.e. pH of -0.2 and -0.5 (Figs. 10(c) and (d)). Irregular and porous structures appeared to be typical for zinc electrodeposits obtained from chloride-containing electrolytes [56]. It was reported that increased amounts of chloride ions in the zinc sulphate solution promoted a charge-transfer during the metal deposition, stimulated nucleation of the zinc crystals and decreased size of the platelet crystals, but also increased dimensions of the concavities formed on the zinc surface [46].

For comparative purposes, few experiments with more alkaline solutions (pH 2.0–2.8) or higher current densities were performed. Figure 11 shows exemplary morphologies of zinc produced in such conditions. It was found that coevolution of hydrogen during electrolysis at higher pH initiated fast alkalization of the electrolyte adjacent to the cathode surface. It favored hydrolysis of zinc ions:

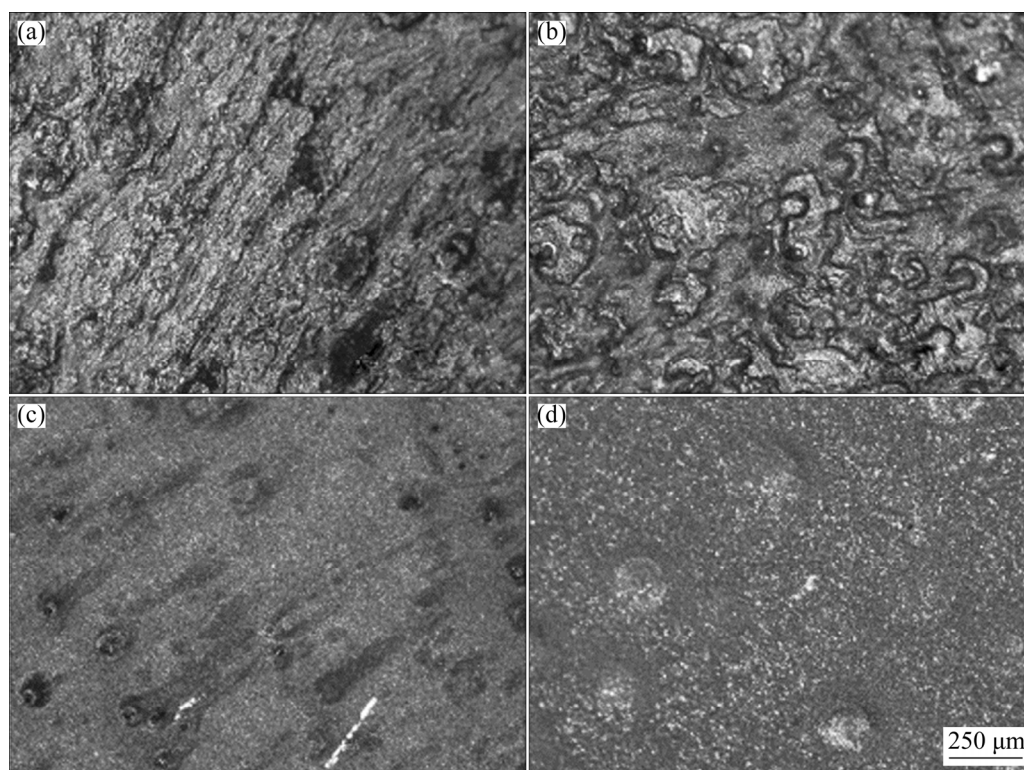


Fig. 10 Surface morphologies of zinc deposited at 5 A/dm² from solutions with various pH: (a) 0.7; (b) 0.1; (c) -0.2; (d) -0.5



and incorporation of white basic zinc sulphate (Figs. 11(a) and (b)) into the deposit (Fig. 12). This gave cathodic current efficiencies as high as $(115 \pm 10)\%$ and electrolysis voltages of 4.2–4.8 V. In turn, higher current densities (8–10 A/dm²) in acidic solutions produced more porous metallic layers (Figs. 11(c) and (d)) with powdery deposit at the substrate edges caused by mass transfer limitations.

The obtained results showed that the zinc

electrowinning was highly effective regardless of chloride ions in the bath. It can change morphology of the deposits, but can also attack lead anodes [19]. The latter may be prevented by an application of more resistant materials [57]. However, recent studies [44] have shown that the presence of manganese ions in the electrolyte can protect the electrodes against corrosion, especially when Mn²⁺/Cl⁻ concentration ratio in the electrolyte ranges from 7 to 11. It is attributed to the deposition of manganese dioxide on the anode surface,

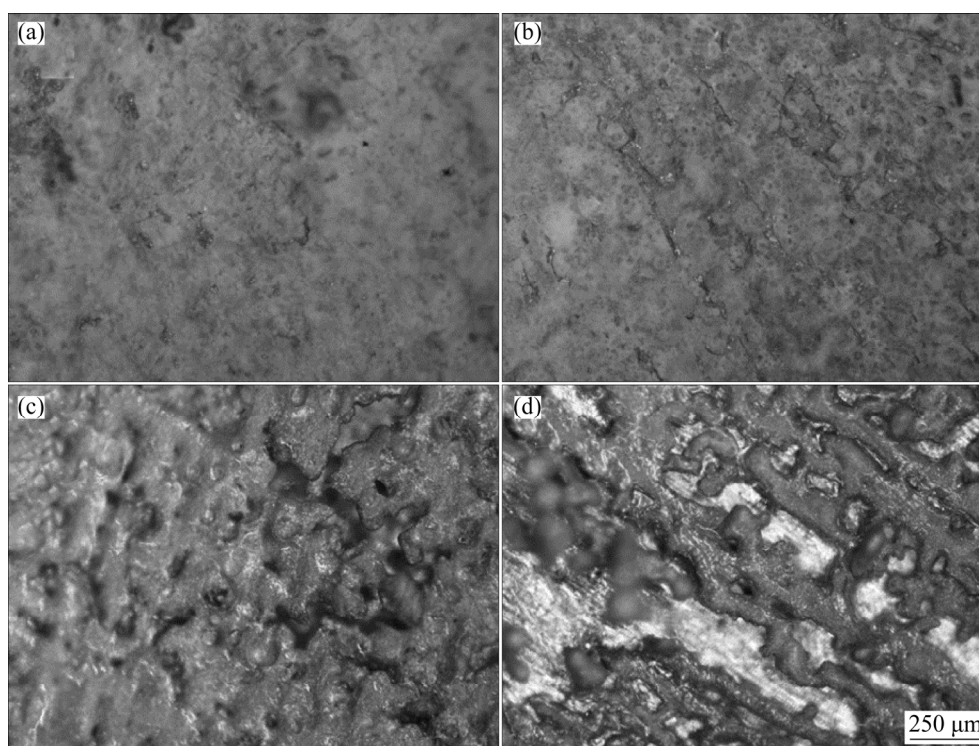


Fig. 11 Morphologies of defective zinc surface produced under different conditions: (a) pH 2.8, 6 A/dm²; (b) pH 2.0, 6 A/dm²; (c) pH 1.0, 8 A/dm²; (d) pH 0.7, 10 A/dm²

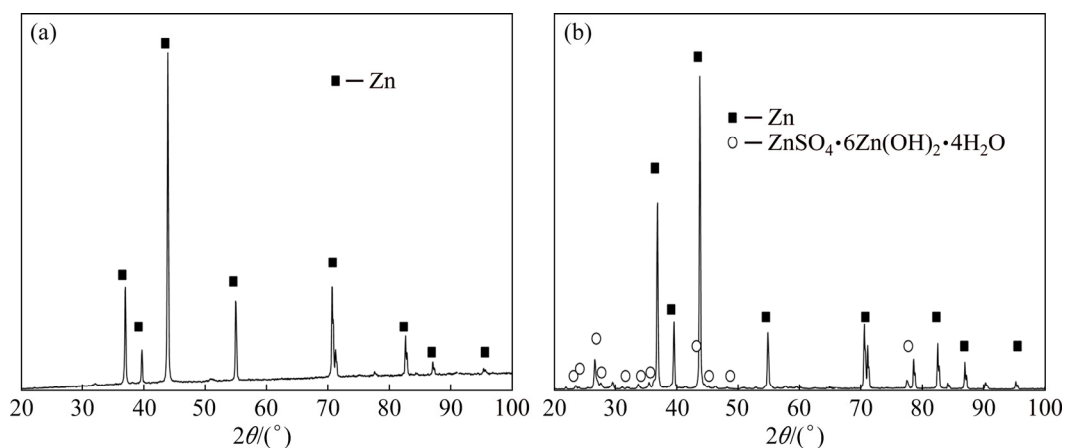


Fig. 12 Exemplary XRD patterns of zinc deposit produced under different conditions: (a) pH 0.1, 5 A/dm²; (b) pH 2.0, 6 A/dm²

producing a diffusion barrier for chlorine oxidation and lead dissolution. This further reduces contamination of the cathodic zinc with lead [30]. However, increasing concentration of manganese sulphate in the electrolyte can decrease the cathodic current efficiency and change the size of the zinc platelets [58]. The optimal concentration of Mn^{2+} ions in the zincous bath is 1–5 g/L [30,43], thus, the level of manganese ions in the investigated electrolyte was acceptable (up to 1 g/L). Nevertheless, it seems to be not enough to eliminate disadvantage action of chloride ions.

4 Conclusions

(1) The zinc ash with a total zinc content of 63% was composed mainly of oxide–chloride zinc compounds with a small fraction of a metallic phase (3.5%).

(2) The material was well leachable in sulphuric acid with the most satisfactory bath loadings no higher than 150 g/L, giving the final concentration of zinc ions up to about 90 g/L. Production of more concentrated zinc sulphate showed to be unreasonable due to problems during subsequent purification stage.

(3) The best alternative of iron elimination from the leaching liquors was gradual dosing of calcium carbonate.

(4) The electrolytic zinc recovery can be carried out from acidic solutions of pH in a range of 0.1–1.0 over a wide range of current densities (3–6 A/dm²) without deterioration of the deposit quality.

(5) The final product can be returned to hot-dip galvanizing process to close zinc loop in-house as it has been shown by implementation of the process in one of the domestic plants.

Acknowledgements

This research work was realized under the Project No. POIR.01.01.01–00–0032/16 in the frame of Smart Growth Operational Programme 2014–2020 financed by the National Centre for Research and Development (Poland).

References

[1] MASS P, PEISSKER P. Handbook of hot-dip galvanization [M]. Weinheim: Wiley, 2011.
 [2] VOURLIAS G, PISTOFIDIS N, PAVLIDOU E,

STERGIOUDIS G, POLYCHRONIADIS E K. Study of the structure of hot-dip galvanizing byproducts [J]. Journal of Optoelectronic Advanced Materials, 2007, 9(9): 2937–2942.
 [3] TRPČEVSKÁ J, HLUCHÁNOVÁ B, VINDT T, ZORAWSKI W, JAKUBÉCZYOVÁ D. Characterization of the bottom dross formed during batch hot-dip galvanizing and its refining [J]. Acta Metallurgica Slovaca, 2010, 16(3): 151–156.
 [4] SCHMITZ D, FRIEDRICH B. In-house recycling of hard zinc and zinc ash by liquid metal centrifugation [C]//Proceedings of EMC. Düsseldorf, Germany: GDMB, 2007: 1–20.
 [5] VOURLIAS G, PISTOFIDIS N, STERGIOUDIS G, POLYCHRONIADIS E K. A negative effect of the insoluble particles of dross on the quality of the galvanized coatings [J]. Solid State Science, 2005, 7(4): 465–474.
 [6] BLAŠKOVÁ K, TRPČEVSKÁ J, PIROŠKOVÁ J, LAUBERTOVÁ M. Zinc waste treatment originated during hot-dip galvanizing [J]. World of Metallurgy—Erzmetall, 2017, 70(4): 223–226.
 [7] BAKARAT M A. Pyrometallurgical processing of zinc ash and flue dust [J]. Acta Metallurgica Slovaca, 2003, 9(4): 259–269.
 [8] SMAKOWSKI T, GALOS K, LEWICKA E. Balance of management of mineral resources of Poland and the world 2013 [M]. Warszawa: Panstwowy Instytut Geologiczny, 2013.
 [9] QYR Steel Research Center. Global hot-dip galvanized steel market insights, forecast to 2025 [M]. Beijing: QYR Steel Research Center, 2019. <https://www.reportsreports.com/reports/1821020-global-hot-dip-galvanized-steel-market-insights-forecast-to-2025.html>.
 [10] AINSLEY M. Improving productivity and quality in the hot dip galvanizing process [EB/OL] [2019–06–08]. <http://www.coezinc.com>.
 [11] BRIGHT M A, DEEM N J, FRYATT J. The advantages of recycling metallic zinc from the processing wastes of industrial molten zinc applications [C]//Light Metals 2007. Orlando, USA: TMS Annual Meeting & Exhibition, 2007: 1–7.
 [12] KATZUNG W, RITTING R. Zinc ash formation and zinc consumption in dependence on parameters of pretreatment in hot dip galvanizing [J]. Metall, 1998, 52(5): 282–291.
 [13] DVOŘÁK P, JANDOVÁ J. Hydrometallurgical recovery of zinc from hot dip galvanizing ash [J]. Hydrometallurgy, 2005, 77: 29–33.
 [14] RUDNIK E, WŁOCH G, SZATAN L. Preliminary investigation on leaching behavior of zinc ash [J]. Archives of Metallurgy and Materials, 2018, 63(2): 801–807.
 [15] RUDNIK E, WŁOCH G, SZATAN L. Hydrometallurgical treatment of zinc ash from hot-dip galvanizing process [J]. Mineral and Metallurgical Processing, 2018, 35(2): 69–76.
 [16] TAKÁCOVÁ Z, HLUCHÁNOVÁ B, TRPČEVSKÁ J. Leaching of zinc from zinc ash originating from hot dip galvanizing [J]. Metall, 2010, 64(12): 517–519.
 [17] TRPČEVSKÁ J, RUDNIK E, HOLKOVÁ B, LAUBERTOVÁ M. Leaching of zinc ash with hydrochloric acid solutions [J]. Polish Journal of Environmental Studies, 2018, 27(4): 1765–1771.

- [18] NIRDOŠ I, KALIA R K, MUTHUSWAMI S V. Bench scale investigations on the electrolytic recovery of zinc powder from Galvanizer's ash [J]. *Hydrometallurgy*, 1988, 20: 203–217.
- [19] NICOL M, AKILAN C, TJANDRAWAN V, GONZALEZ J A. The effects of halides on the electrowinning of zinc II. Corrosion of lead–silver anodes [J]. *Hydrometallurgy*, 2017, 173: 178–191.
- [20] TAKADA T, KIYAMA M, TORII H, ASAI T, TAKANO M, NAKANISHI M. Effect of pH values on the formation and solubility of zinc compounds [J]. *Bulletin of the Institute for Chemical Research*, 1978, 56(5): 242–246.
- [21] RUDNIK E. Recovery of zinc from zinc ash by leaching in sulphuric acid and electrowinning [J]. *Hydrometallurgy*, 2019, 188: 256–263.
- [22] LIDE D R. *CRC handbook* [M]. 84th edition. Boca Raton, Florida: CRC Press, 2003.
- [23] ŞAHİN F C, DERİN B, YÜCEL O. Chloride removal from zinc ash [J]. *Scandinavian Journal of Metallurgy*, 2000, 29: 224–230.
- [24] TRPČEVSKÁ J, HOLKOVÁ B, BRIANČIN J, KORÁLOVÁ K, PIROŠKOVA J. The pyrometallurgical recovery of zinc from the coarse-grained fraction of zinc ash by centrifugal force [J]. *International Journal of Mineral Processing*, 2015, 143: 25–33.
- [25] GÜRESİN N, TOPKAYA Y A. Dechlorination of a zinc dross [J]. *Hydrometallurgy*, 1998, 49: 179–187.
- [26] GOSTU S, MISHRA D, SAHU K K, AGRAWAL A. Precipitation and characterization of zinc borates from hydrometallurgical processing of zinc ash [J]. *Materials Letters*, 2014, 134: 198–201.
- [27] DAKHILI N, RAZAVIZADEH H, SALEHI M T, SEYEDEIN S H. Recovery of zinc from the final slag of steel's galvanizing process [J]. *Advanced Materials Research*, 2011, 264–265: 592–596.
- [28] MURESAN L, MAURIN G, ONICIU L, GAGA D. Influence of metallic impurities on zinc electrowinning from sulphate electrolyte [J]. *Hydrometallurgy*, 1996, 43: 345–354.
- [29] TJANDRAWAN V, NICOL M J. Electrochemical oxidation of iron(II) ions on lead alloy anodes [J]. *Hydrometallurgy*, 2013, 131–132: 81–88.
- [30] ZHANG Wen-sheng, CHENG Chu-yong. Manganese metallurgy review. Part III: Manganese control in zinc and copper electrolytes [J]. *Hydrometallurgy*, 2007, 89: 178–188.
- [31] DUTRIZAC J E. Calcium sulphate solubilities in simulated zinc processing solutions [J]. *Hydrometallurgy*, 2002, 65: 109–135.
- [32] ROBIE R A, HEMINGWAY B S. *Thermodynamic properties of minerals and related substances at 298.15 K and 1 bar (10⁵ Pascals) pressure and at higher temperatures* [M]. Washington: United States Government Printing Office, 1995.
- [33] HAGEMANN S. *Development of a thermodynamic model for zinc, lead and cadmium in saline solutions* [M]. Berlin: GRS, 2012.
- [34] LIU H X, PAPANGELAKIS V G. Thermodynamic equilibrium of the O₂–ZnSO₄–H₂SO₄–H₂O system from 25 to 250 °C [J]. *Fluid Phase Equilibria*, 2005, 234: 122–130.
- [35] PILLAY P. Overcoming interference from hydrolysable cations during the determination of sulphuric acid by titration [D]. Pretoria: University of Pretoria, 2000.
- [36] MONAHOV B, PAVLOV D, KIRCHEV A, VASILEV S. Influence of pH of H₂SO₄ solution on the phase composition of the PbO₂ active mass and of the PbO₂ anodic layer formed during cycling of lead electrodes [J]. *Journal of Power Sources*, 2003, 113: 281–291.
- [37] MYHRE C E L, CHRISTENSEN D H, NICOLAISEN F M, NIELSEN C J. Spectroscopic study of aqueous H₂SO₄ at different temperatures and compositions: Variations in dissociation and optical properties [J]. *Journal of Physical Chemistry A*, 2003, 107: 1979–1991.
- [38] CASAS J M, CRISOSTOMO G, CIFUENTES L. Aqueous speciation of Fe(II)–Fe(III)–H₂SO₄ systems at 25 and 50 °C [J]. *Hydrometallurgy*, 2005, 80: 254–264.
- [39] WANG W, DRESINGER D. The acid-base behavior of zinc sulfate electrolytes: The temperature effect [J]. *Metallurgical and Materials Transactions B*, 1998, 29: 1157–1166.
- [40] MCCARTY C G, VITZ E. pH paradoxes: Demonstrating that it is not true that pH=–log[H] [J]. *Journal of Chemical Education*, 2006, 83(5): 752–757.
- [41] ROLIA E, DUTRIZAC J E. The determination of free acid in zinc processing solutions [J]. *Canadian Metallurgical Quarterly*, 1984, 23(2): 159–167.
- [42] DINARDO O, DUTRIZAC J E. The solubility of silver chloride in sulphate media [J]. *Hydrometallurgy*, 1991, 26: 47–59.
- [43] ABBEY C E, JIN W, MOATS M S. Manganese–chloride interactions on Pb–Ag anode behaviour in synthetic sulfuric acid electrolytes [C]//*Extraction 2018*. Heidelberg: Springer, 2018: 1521–1533.
- [44] KASHIDA K, OUE S, NAKANO H. Effect of chloride ions in electrowinning solutions on zinc deposition behavior and crystal texture [J]. *Materials Transactions*, 2017, 58(10): 1418–1426.
- [45] XIAO Hui-fang, CHEN Qing, CHENG Huan, LI Xiu-min, QIN Wen-meng, CHEN Bao-sheng, XIAO Dong, ZHANG Wei-ming. Selective removal of halides from spent zinc sulfate electrolyte by diffusion dialysis [J]. *Journal of Membrane Science*, 2017, 537: 111–118.
- [46] ISMAEL M R C, CARVALHO J M R. Iron recovery from sulphate leach liquors in zinc hydrometallurgy [J]. *Minerals Engineering*, 2003, 16: 31–39.
- [47] KRUPKA D, OCHAB B, MIERNIK J. *The Boleslaw electrolytic zinc plant [C]//Lead–Zinc 2000*. New York: TMS, 2000: 277–288.
- [48] SVENS K. Outotec atmospheric zinc concentrate direct leaching process—past, present and future [J]. *World of Metallurgy—Erzmetall*, 2010, 63(3): 136–141.
- [49] HERRERO D, ARIAS P L, CAMBRA J F, ANTUÑANO N. Studies on impurity iron removal from zinc electrolyte using MnO₂–H₂O₂ [J]. *Hydrometallurgy*, 2011, 105: 370–373.
- [50] BARAKAT M A, MAHMOUD M H H, SHEHATA M. Hydrometallurgical recovery of zinc from fine blend of galvanization processes [J]. *Separation Science and Technology*, 2006, 41: 1757–1772.
- [51] GUERRA E, BESTETTI M. Physicochemical properties of ZnSO₄–H₂SO₄–H₂O electrolytes of relevance to zinc

- electrowinning [J]. Journal of Chemical Engineering Data, 2006, 51: 1491–1497.
- [52] ZENG De-wen, WANG Wen-lei. Solubility phenomena involving CaSO_4 in hydrometallurgical processes concerning heavy metals [J]. Pure Applied Chemistry, 2011, 83(5): 1045–1061.
- [53] ALFANTAZI A M, DRESINGER D B. The role of zinc and sulfuric acid concentrations on zinc electrowinning from industrial sulfate based electrolyte [J]. Journal of Applied Electrochemistry, 2001, 31: 641–646.
- [54] GUILLAUME P, LECLERC N, BOULANGER C, LECUIRE J M, LAPICQUE F. Investigation of optimal conditions for zinc electrowinning from aqueous sulfuric acid electrolytes [J]. Journal of Applied Electrochemistry, 2007, 37: 1237–1243.
- [55] ANTUÑANO N, HERRERO D, ARIAS P L, CAMBRA J F. Electrowinning studies for metallic zinc production from double leached Waelz oxide [J]. Process Safety and Environmental Protection, 2013, 91: 495–502.
- [56] BAIK D S, FRAY D J. Electrodeposition of zinc from high acid zinc chloride solutions [J]. Journal of Applied Electrochemistry, 2001, 31: 1141–1147.
- [57] RAMACHANDRAN P, NANDAKUMAR V, SATHAIYAN N. Electrolytic recovery of zinc from zinc ash using a catalytic anode [J]. Journal of Chemical Technology and Biotechnology, 2004, 79: 578–583.
- [58] MACKINNON D J, BRANNEN J M. Effect of manganese, magnesium, sodium and potassium sulphates on zinc electrowinning from synthetic acid sulphate electrolytes [J]. Hydrometallurgy, 1991, 27: 99–111.

从工业热浸镀锌灰中湿法回收锌

Ewa RUDNIK

Faculty of Non-ferrous Metals, AGH University of Science and Technology,

Al. Mickiewicza 30, 30-059 Cracow, Poland

摘要: 研究热浸镀锌厂的锌灰, 使之可以作为二次锌资源返回镀锌槽。这种废料中含有 63% 的锌, 锌以金属、氧化物和羟基氯化物相存在。在各种浸出槽负荷(100~300 g/L)下于 H_2SO_4 溶液(20%, 25%)中浸出锌灰, 研究锌、锰、铁和氯离子的浸出行为。考察几种从浸出液中除铁的方法。添加絮凝剂对后续的铁沉淀物过滤有害, 因为会导致溶液黏度增大; 氧化锌与为了提高 pH 值而加入的碳酸钙结合, 形成高密度的悬浊液, 无法从硫酸锌溶液中分离出来。在不同的 pH 值(-0.5~2.8)下进行锌电积, 电流密度范围为 3~10 A/dm^2 。从锌灰中回收纯金属的最佳条件如下: 用 20% 的硫酸浸出, 浸出槽负荷 100~150 g/L, 用 H_2O_2 和 CaCO_3 沉淀出 $\text{Fe}_2\text{O}_3 \cdot x\text{H}_2\text{O}$, 在 pH 0.1~1.0、电流密度 3~6 A/dm^2 的条件下进行电积锌。还讨论电解液中 pH 与游离 H_2SO_4 浓度之间的关系。锌电解液的 pH-酸浓度曲线介于纯 H_2SO_4 溶液的实验曲线与计算曲线之间; 如果溶液中存在铁离子, 则曲线向低 pH 方向移动。

关键词: 锌灰; 锌; 浸出; 净化; 电积; 回收利用

(Edited by Wei-ping CHEN)